IEEE Access
Multidisciplinary ⁝ Rapid Review ⁝ Open Access Journal

Received 8 May 2025, accepted 8 June 2025, date of publication 17 June 2025, date of current version 26 June 2025.

Digital Object Identifier 10.1109/ACCESS.2025.3580660

RESEARCH ARTICLE

Detailed Design of Lattice Tower for Low Speed Wind Turbines

JAMES ROJAS WATERHOUSE[1], CARLOS HENRIQUE GASPARETTI[2], KAUAN PIRES QUEVEDO[2,3], AND GUILHERME BEPPU DE SOUZA[2]

[1]Department of Aeronautical Engineering, University of São Paulo, São Carlos, São Paulo 13566-590, Brazil
[2]Newco Blades Technology, São Carlos, São Paulo 13565-261, Brazil
[3]Department of Mechanical Engineering, University of São Paulo, São Carlos, São Paulo 13566-590, Brazil

Corresponding author: James Rojas Waterhouse (james@sc.usp.br)

This work was supported by the Eletrobras Furnas and Agência Nacional de Energia Elétrica (ANEEL) under Grant PD-00394-19004/2019.

ABSTRACT This study presents the design of a lattice tower for wind turbines with a downwind rotor configuration, intended for operation in low-intensity wind conditions (Class III-B, according to IEC 61400-1). Developed as part of the ABV/Furnas project, the analysis outlines the criteria used to define the optimal tower typology, considering structural, aerodynamic, and economic factors. A key challenge in downwind rotor turbines is the wake generated by the flow around the tower, which can negatively affect rotor performance. To address this, a lattice tower with aerodynamic-profiled members was selected. This solution not only reduces aerodynamic interference but also lowers manufacturing, transportation, and assembly costs. The study demonstrates the feasibility and innovations of this approach. It highlights how lattice structures reduce aerodynamic impact, enhancing rotor efficiency. The analysis covers essential structural and geometric parameters, including weight, wind blocking area, ground loading, and their influence on foundation costs. Additionally, the effect of tower geometry on its natural vibration frequency is examined to prevent resonance and ensure long-term structural stability. Various lattice tower configurations are compared to conventional tubular towers, assessing their technical performance. Logistical constraints – such as transportation feasibility, on-site assembly, and limitations of the Brazilian steel market – are also evaluated, ensuring the practicality and cost-effectiveness of the proposed design for deployment in Brazil.

INDEX TERMS Lattice tower, wind turbines, downwind rotor configuration, aerodynamic performance, wake effect, tower typology.

I. INTRODUCTION

Wind energy accounts for about 15.8% of Brazil's energy matrix [1], but the wind turbines currently used in the country, designed for European and North American markets, are not optimized for the low-intensity wind conditions that predominate in most of Brazil. The Low-Speed Wind Turbine (*Aerogerador de Baixa Velocidade* - ABV) project aims to address this issues by developing turbines adapted to the wind conditions characteristics of Brazilian regions with low wind intensity. With wind energy production concentrated in the northeast and the highest energy demand in the southeast, which accounts for 42% of the population and 53% of the GDP [2], [3], the ABV seeks to increase the efficiency and economic viability of wind energy generation in high-demand areas, reducing dependence on long-distance transmission and promoting a better use of Brazil's wind potential.

The ABV low-speed wind-turbine prototype is designed to be economically viable at IEC Class III-B sites (characterized by an annual mean wind speed of approximately 7.5 m/s and a 10-minute, 50-year extreme gust of 52.5 m/s [4], [5]). It delivers its full 250 kW output from just above 5 m/s – a much broader low-wind band than conventional turbines, which typically reach rated power only at 10-15 m/s [6].

Its two 38 m downwind blades are molded from advanced composites and feature airfoils optimized for low-Reynolds-number flows, minimizing cyclic loading under light winds. The cast-iron hub incorporates a teetered oscillating coupling

The associate editor coordinating the review of this manuscript and approving it for publication was Rosario Pecora.

that dampens torsional shocks before torque is stepped up through the gearbox to a high-speed synchronous generator – maximizing conversion efficiency and reducing mechanical fatigue.

This study presents a comprehensive methodology for the development and design of the support tower for a low-speed, downwind wind turbine, addressing the structural, aerodynamic, and economic factors essential for practical deployment.

Considering cost concerns, the manufacturing and installation of onshore wind projects represent the primary cost components in wind energy development, accounting for 64-84% of the total installed cost [7]. For reduced-rated machines, the turbine alone typically accounts for 40% to over 50% of the total project cost, with the tower being the largest single contributor [8]. The tower alone consumes approximately 26.6% of the total turbine expenditure, according to WindEurope [8], [9], and about 24% of project labor resources [10]. Logistics further amplify these outlays, since heavier segments, greater hub heights, and longer haul distances all drive up transport and erection costs [10]. These figures underscore the tower's pivotal role in overall project economics and highlight the importance of strategies aimed at reducing both fabrication and installation expenses.

A specific challenge of the ABV's downwind layout is the tower's turbulent wake – or "tower shadow" – thrown onto the rotor, degrading blade lift, increasing acoustic emissions, and inducing unsteady loads that accelerate fatigue damage [11], [12], [13], [14]. Mitigating this aerodynamic interference is therefore essential to maximize energy capture, suppress noise, and ensure operational stability.

In light of these challenges, the main objectives in the tower's design are twofold: (i) attenuate tower-induced flow disturbances to boost efficiency, reduce noise, and extend component fatigue life, and (ii) streamline tower fabrication, transport, and erection to lower CapEx (capital expenditure) while rigorously preserving structural integrity and aerodynamic performance. By addressing these aerodynamic and economic levers in tandem, the proposed methodology delivers ABV towers that are both performance-robust and cost-competitive, advancing the viability of downwind wind-energy installations and supporting broader renewable-energy adoption.

To meet these objectives, the project proposes the use of a lattice tower with aerodynamic profiles, a solution that minimizes aerodynamic interference and reduces manufacturing, transportation, and assembly costs when compared to traditional tubular towers. The methodology includes analyzing the ideal tower typology and using finite element analysis (FEA) to evaluate structural and aerodynamic behavior in compliance with international standards.

II. TOWER MODEL DEVELOPMENT

To address the aerodynamic and economic challenges of the ABV's downwind design, this section outlines the development of a lattice tower model optimized for Class III-B wind conditions (IEC 61400-1 [5]).

Loads were analyzed per IEC 61400-1 [5] and NBR standards to identify the critical design scenario. The tower's cross-section was designed to ensure structural integrity under these conditions. Finite element analysis (FEA) was employed to validate the design, while the lattice typology was optimized to minimize weight, aerodynamic interference, and foundation costs. The tower geometry was also analyzed to ensure its natural frequency avoids resonance, enhancing long-term stability.

The design of tower components, including fasteners and joints, prioritized structural integrity and ease of assembly, addressing logistical challenges such as transportation constraints in Brazil.

This process yielded a lattice tower design that reduces the tower shadow effect, lowers fabrication and installation costs, and ensures feasibility for low-wind regions in Brazil, with detailed analyses presented in the following sections.

A. LOAD SPECTRUM ANALYSIS

To ensure the structural integrity of the ABV's lattice tower under Class III-B wind conditions, this section details the load spectrum analysis based on IEC 61400-1 [5] and NBR 6123 [15] standards. The tower is subjected to gravitational, inertial, aerodynamic, operational, and additional loads (e.g., startup, impact, ice accumulation).

The IEC 61400-1 standard [5] provides a comprehensive framework for load case analysis, specifying wind condition models, safety factors, and design requirements for normal and extreme operating conditions. Additionally, wind loads on the tower were calculated per NBR 6123 [15], which defines methodologies for determining wind pressures based on local conditions, terrain characteristics, and structural geometry. This integrated approach ensures a robust and regionally compliant load assessment.

1) CRITICAL SCENARIO

The critical design scenario was identified as the turbine in a parked state under extreme wind conditions with a 50-year recurrence period, combined with a loss of electrical network connection. This condition subjects the tower to maximum wind loads without active control, making it decisive for structural design.

a: EXTREME WIND MODEL (IEC 61400-1)

The extreme wind speed, v_{e50}, was calculated using the IEC 61400-1 [5] steady wind model:

$$v_{e50}(z) = 1.4 \cdot V_{\text{ref}} \left(\frac{z}{z_{\text{hub}}}\right)^{0.11} \tag{1}$$

where:

- $V_{\text{ref}} = 37.5$ m/s, the reference wind speed for a Class III turbine;

- z_{hub}, the hub height;
- z, the height above ground.

Using OpenFAST, loads were computed for a wind speed of 52.5 m/s at hub height, with blades feathered and the rotor stationary at a 0-180° orientation, simulating the loss of electrical connection. A partial safety factor of 1.35 was applied to the nominal load (F_k) to obtain the design load (F_d) per IEC 61400-1 [5]:

$$F_d = 1.35 \cdot F_k \tag{2}$$

b: WIND LOADING (NBR 6123)

Wind loads on the tower were calculated per NBR 6123 [15], starting with the dynamic pressure:

$$q = 0.613 \cdot V_k^2 \tag{3}$$

where:

$$V_k = V_0 \cdot S_1 \cdot S_2 \cdot S_3 \tag{4}$$

and:

- V_0, the 3-second gust speed with a 50-year recurrence period;
- S_1, the topographic factor (assumed 1.0 for flat terrain);
- S_2, the terrain roughness factor (0.9 for open terrain);
- S_3, the statistical factor (1.1, reflecting the tower's safety role).

The drag force was then computed as:

$$F_a = C_a \cdot q \cdot K \cdot L \cdot d \tag{5}$$

where:

- C_a, the drag coefficient, dependent on the geometry interacting with air;
- K, a reduction factor based on L/d;
- L, the bar length;
- d, the bar's frontal dimension facing the wind direction.

This analysis identified peak loads under the critical scenario, guiding the subsequent structural design of the ABV tower.

B. STRUCTURAL MODELING

Using the calculated loads acting on the tower, the design begins with estimating member forces, followed by determining minimum cross-sections for structural components, adhering to international standards. Initial estimates use simplified truss analysis models, typically in 2D, to understand load distribution. These results are refined through finite element models (FEA), enabling comprehensive analysis of the structure's response. Following the sequence of design phases ensures a logical progression, minimizing errors and optimizing the final design.

1) MINIMUM CROSS-SECTION DESIGN

The cross-sections of tower components were designed per standards including IEC 61400-2 [16], NBR 8800 [17], ASCE 7 [18], and IEC 61400-3 [19], using the Load and Resistance Factor Design (LRFD) methodology. These standards incorporate safety factors to address uncertainties in load estimation, material properties, and structural behavior, ensuring reliability under diverse conditions such as wind, earthquakes, and manufacturing variations. IEC 61400-2 provides guidelines for steel structures, NBR 8800 specifies Brazilian requirements for steel and composite structures, ASCE 7 defines minimum design loads, and IEC 61400-3 governs welding quality. Cross-sections were designed to meet criteria for bending, shear, and fatigue resistance, forming a robust framework for the ABV tower.

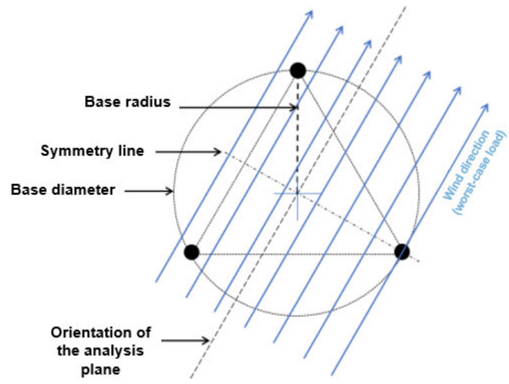

FIGURE 1. Selected analysis plane for a three-column tower, parallel to the wind direction that generates the critical aerodynamic load from the rotor.

2) FINITE ELEMENT MODELS

Finite element analysis (FEA) was employed to validate and refine the preliminary design, progressing from a 2D model for initial analysis to a 3D model for detailed validation.

a: 2D MODEL

In the preliminary phase, a 2D model was developed to estimate member forces, leveraging structural symmetries and projecting primary loads onto a single plane. The analysis plane, parallel to the wind direction causing the critical aerodynamic load from the rotor, is shown in Figure 1. Secondary forces and moments outside this plane were neglected due to their lower intensity. Wind loads acting directly on the tower were excluded in this phase but will be included in 3D FEA for conceptual and detailed design. Figure 2 illustrates the 2D FEA model for a three-column tower.

b: 3D MODEL

The 3D FEA, conducted in ANSYS, improved the accuracy of stress and modal predictions compared to the 2D model, particularly for stress concentrations and fatigue analysis. While 2D FEA offers rapid assessment of global stresses, it cannot capture localized effects at joints or complex geometries. The 3D FEA used a two-stage approach to balance accuracy and computational cost:

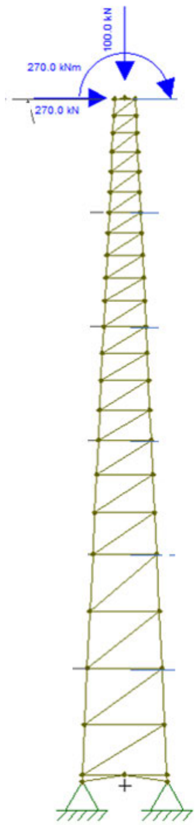

FIGURE 2. 2D FEA model for preliminary structural analysis.

- **Simplified Beam Element Model:** A coarse model with Timoshenko beam elements simulated global behavior and identified critical load cases, reducing the need for extensive 3D analyses.
- **Detailed 3D Meshed Model:** A refined model with 8-node solid elements (10 mm mesh size) was used for critical cases, accurately capturing stress concentrations at bolted joints and geometric discontinuities.

The 3D model provided precise stress and strain estimates at critical points, ensuring compliance with safety and fatigue requirements. Figure 3 show the beam and solid element meshes, highlighting the increased detail in the 3D model.

3) JOINTS DESIGN

For the ABV's lattice tower, joint design ensures structural performance while addressing logistical constraints in Brazil. Joints connect truss components, requiring careful design to ensure stability, load transfer, and ease of assembly, transportation, and maintenance. The design considered welded, bolted, and pinned connections, each adhering to relevant standards. Welded joints were designed per AWS D1.1 [19], ensuring weld quality and durability. Bolted and pinned connections followed Eurocode 3, Part 1-8 [20], with designs optimized for shear and tensile resistance under critical load cases. Bolted connections were prioritized to facilitate on-site assembly, aligning with Brazil's transportation limitations.

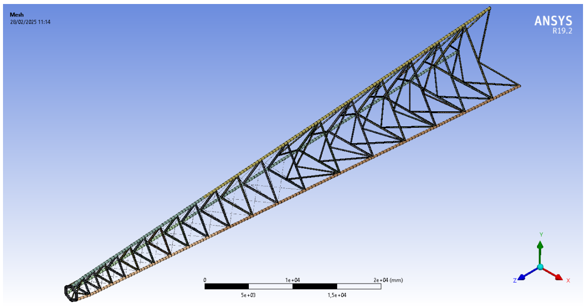

(a) Complete tower model.

(b) Joint region.

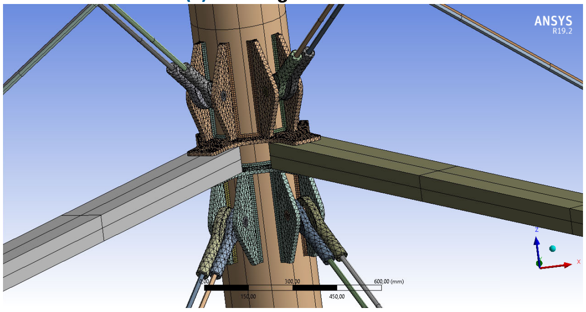

(c) Weld and hardpoint mesh.

FIGURE 3. 3D solid element model of the tower.

C. COMPARATIVE ANALYSIS FOR OPTIMAL TOWER TOPOLOGY DETERMINATION

To determine the optimal tower topology for the ABV wind turbine under Class III-B wind conditions, a comparative analysis evaluated lattice tower configurations (3, 4, 5, and 6 columns; base diameters of 5.66, 7.08, 9.90, 14.14, and 18.38 m) against a circular tower (3.2 m base diameter). The analysis considered structural weight, aerodynamic performance, and foundation costs, with the top diameter fixed at 2.4 m. Loads were estimated using aeroelastic software (OpenFAST) simulating the critical scenario: a parked turbine under extreme wind conditions (52.5 m/s, 50-year recurrence) with blade pitch failure, as defined in Section II-A1. Structural design used NBR 8261 Grade C steel (yield strength 345 MPa).

1) STRUCTURAL WEIGHT ANALYSIS

The structural weight is a key factor in manufacturing costs and logistical feasibility. A simplified truss model and LRFD

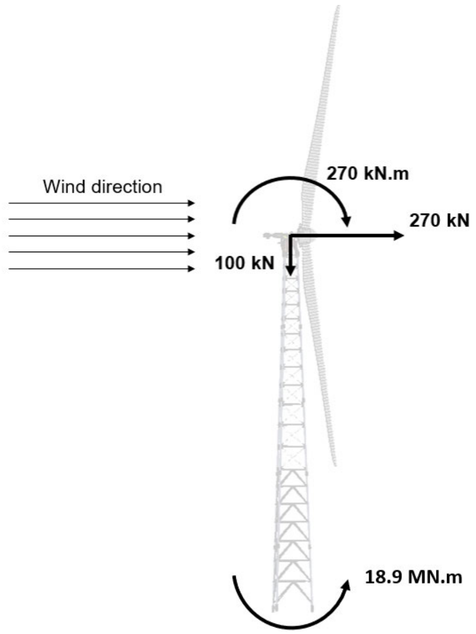

FIGURE 4. Main loads acting on the tower in the ultimate limit state.

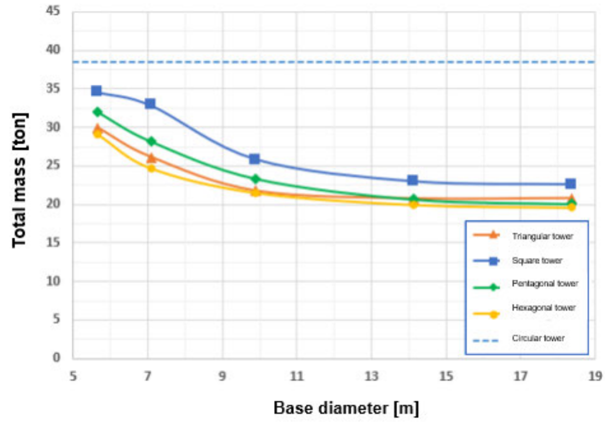

FIGURE 5. Mass comparison of lattice towers with the circular tower.

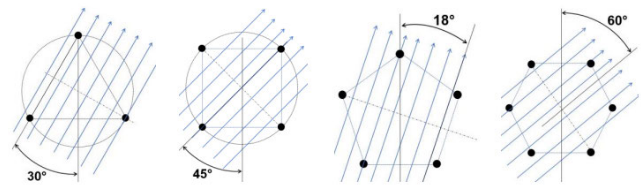

FIGURE 6. Critical wind direction for the analyzed tower configurations.

methodology were employed to estimate the weight of the tower, ensuring it could safely withstand the primary loads. The design calculations were based on NBR 8261 Grade C steel (yield strength of 345 MPa), with the allowable stress determined as:

$$\sigma_{\text{allow}} = \frac{\Phi \cdot F_y}{\text{LF}} = \frac{0.9 \cdot 345}{1.6} = 194\,\text{MPa} \tag{6}$$

The loads considered in the analysis included drag (270 kN), nacelle/rotor weight (100 kN), top moment (270 kN ·m), and base moment (18.9 MN ·m), as shown in Figure 4.

The diameters and thicknesses of the vertical and horizontal tubes were chosen from national manufacturers' catalogs, prioritizing profiles with continuous manufacturing, as some tube dimensions are only produced on-demand in large batches. For the diagonal elements, steel cables were selected to provide the required tension strength while minimizing weight.

In terms of structural optimization, increasing the base diameter from 5.66 meters to 9.9 meters resulted in a 25% reduction in weight, attributed to the enhanced moment of inertia which improved the tower's resistance to bending. However, beyond 12 meters, the weight reduction plateaued, as larger member cross-sections were required to meet buckling constraints.

Among the configurations analyzed, the 6-column tower was the lightest, but the 3-column tower with a 9.9-meter base offered the best balance of cost-effectiveness and structural performance. This configuration proved to be the most efficient in terms of both weight reduction and cost, making it the preferred option.

2) AERODYNAMIC PERFORMANCE

The tower's frontal area affects aerodynamic loads on downwind blades, influencing blade lift, noise, and fatigue. The average frontal area (AF_m) was computed as:

$$AF_m = \frac{\int_0^{\theta_r} A(\theta)\, d\theta}{\theta_r} \tag{7}$$

where θ_r is the angular period (60° for triangular, 90° for square, 36° for pentagonal, 120° for hexagonal). Critical wind directions, inducing the highest member forces, were identified (Figure 6), with 3- and 5-column towers peaking when one column was unloaded, and 4- and 6-column towers peaking with two unloaded columns.

A detailed analysis of the tower's frontal area was conducted to evaluate its aerodynamic impact, assessing minimum, intermediate, and maximum frontal areas across various base diameters and, subsequently, evaluating the variation of frontal area across different wind directions for each base diameter. This analysis revealed periodic variations in frontal area as a function of wind direction, influenced by the tower's geometric configuration. The triangular tower exhibited the lowest average frontal AF_m across all base diameters, minimizing flow disturbance compared to the circular tower (Figure 7).

3) FOUNDATION DESIGN AND COST ANALYSIS

Two foundation models were compared: a lattice tower foundation (square column, 0.25 m^2 cross-section, with square footing, side length L_s, thickness 0.5 m, 45° soil cut, depth h, Figure 8) and a circular tower gravity base (lateral

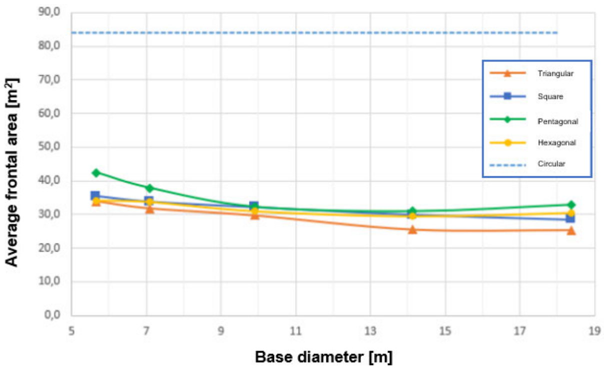

FIGURE 7. Average frontal areas of lattice towers compared to a circular tower (3.2 m diameter).

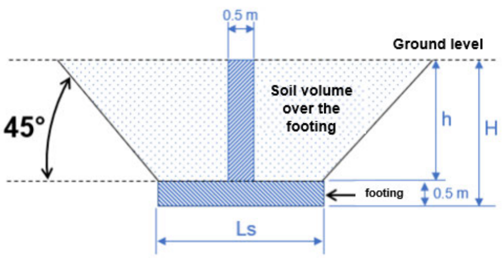

FIGURE 8. Foundation model for lattice towers.

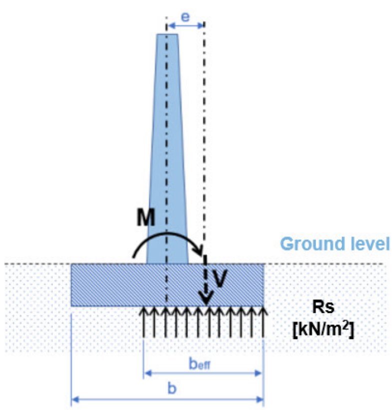

FIGURE 9. Gravity base model for circular tower.

dimension b, Figure 9). A safety factor of 2 was applied to normal loads.

For lattice towers, tensile resistance balanced the normal force ($F_{N\max}$) with concrete and soil weight:

$$2 \cdot F_{N\max} = [(V_s \cdot \rho_s) + (V_c \cdot \rho_c)] \cdot g \tag{8}$$

where $V_s = \left[L_s + \frac{h}{\tan 45^\circ}\right]^2 \cdot h - 0.25 \cdot h$, $V_c = 0.25 \cdot h + 0.5 \cdot L_s^2$, $\rho_s = 2000\,\text{kg/m}^3$, $\rho_c = 2500\,\text{kg/m}^3$, and $g = 9.81\,\text{m/s}^2$. Compressive resistance was:

$$R_s = \frac{2 \cdot F_{N\max}}{L_s^2} \tag{9}$$

with $R_s = 150\,\text{kN/m}^2$.

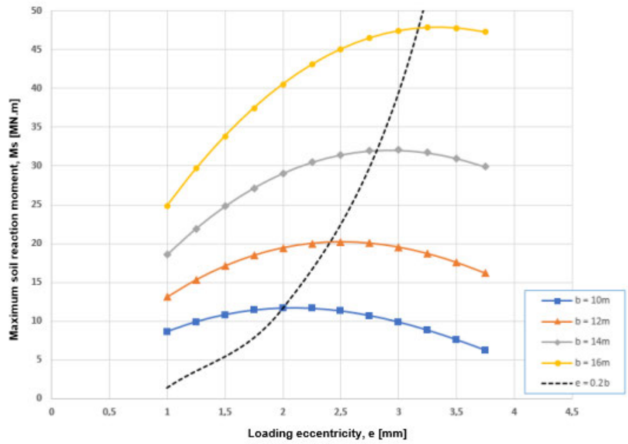

FIGURE 10. Estimated maximum soil reaction capacity for $R_S \approx 150\,\text{kN/m}^2$.

TABLE 1. Reference values for foundation cost calculations.

Parameter	Value
Soil density (ρ_s)	2000 kg/m³
Concrete density (ρ_c)	2500 kg/m³
Soil compressive strength (R_s)	150 kN/m²
Concrete cost	400 R$/m³
Reinforcement cost	4 R$/kg
Soil handling cost	40 R$/m³

For circular towers, the gravity base resisted overturning moment M, with effective area $A_{\text{eff}} = b_{\text{eff}}^2$ for square bases or $A_{\text{eff}} = 2\left[R^2 \cdot \cos^{-1}\left(\frac{e}{R}\right) - e \cdot \sqrt{R^2 - e^2}\right]$ for circular bases. The moment was:

$$M = e \cdot V = e \cdot R_s \cdot A_{\text{eff}} \tag{10}$$

with eccentricity $e < 0.3b$, optimal at $e \approx 0.2b$ (Figure 10).

Foundation costs were estimated using concrete (400 R$/m^3), reinforcement (150 kg/m^3, 4 R$/kg), and soil excavation (40 R$/m^3) (Table 1). Normal loads decreased with larger base diameters and more columns (Figure 11). A foundation depth of 3 m minimized costs for lattice towers (Figures 12a to 12b). The circular tower's gravity base (14.8 m diameter, 1.5 m thickness, 258 m^3 concrete) was designed for a 37.8 MN·m moment. Lattice towers with 10-12 m base diameters cost approximately half as much as the circular tower, with the triangular configuration being the most economical (Figure 13).

III. RESULTS

A. OPTIMAL CONFIGURATION

The triangular lattice tower with a 10-12 m base diameter emerged as the optimal configuration, achieving:

- **Weight**: 40% lower weight, reducing manufacturing and transport costs.
- **Aerodynamic Performance**: 60% smaller frontal area compared to a circular tower, minimizing blade load fluctuations and tower shadow effects.

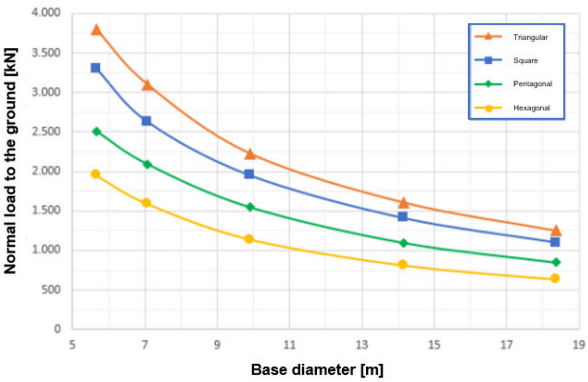

FIGURE 11. Maximum normal loads on the ground for each tower configuration.

TABLE 2. Maximum forces from 2D and 3D FEA for lattice towers (9.9 m base diameter).

No. of Pillars	2D Load [kN]	3D Load [kN]	Difference [%]
3	2230	2149	3.8
4	1950	1850	5.4
5	1550	1423	8.9
6	1140	1075	6.0

TABLE 3. First-mode vibration frequencies of analyzed towers.

Tower Type	1st Mode Frequency [Hz]
Circular (3.2 m)	0.63
Triangular (9.9 m)	0.99
Square (9.9 m)	1.05
Pentagonal (9.9 m)	1.03
Hexagonal (9.9 m)	1.12

- **Foundation Costs**: Approximately 50% lower than the circular tower due to reduced concrete and excavation volumes.

This configuration balances structural efficiency, aerodynamic performance, and economic viability, making it ideal for the ABV's downwind design in Brazil's low-wind regions.

B. STRUCTURAL PERFORMANCE

For the selected triangular lattice tower (9.9 m base diameter), FEA confirmed consistent load paths, with axial load distribution shown in Figure 14. Maximum forces differed by 3.8-8.9% between 2D and 3D models (Table 2). Modal analysis determined the first-mode vibration frequencies, ensuring they are distant from the blade passing frequency (0.7 Hz for a 21 rpm, two-blade turbine). A 6-ton mass was assumed at the tower top (nacelle, rotor, subsystems). Table 3 lists the frequencies, showing that lattice towers achieve 40-60% margins above the blade passing frequency, while the circular tower's frequency (0.63 Hz) is critically close, risking resonance.

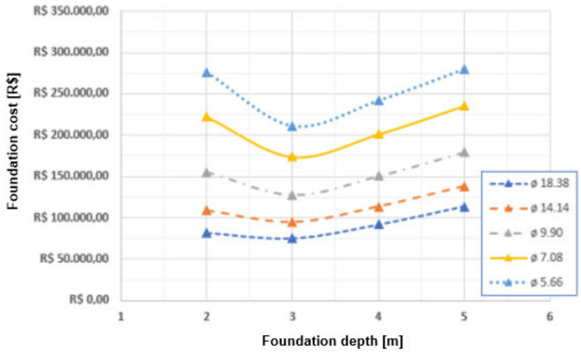

(a) Triangular

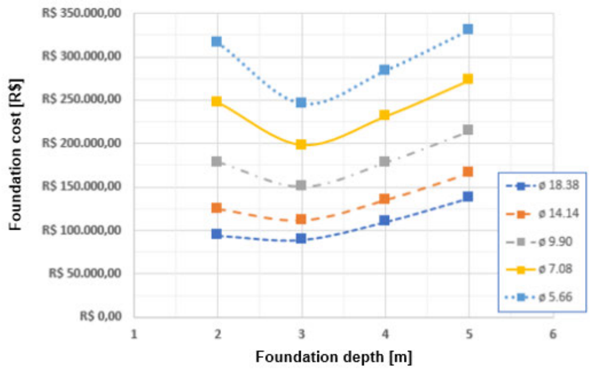

(b) Square

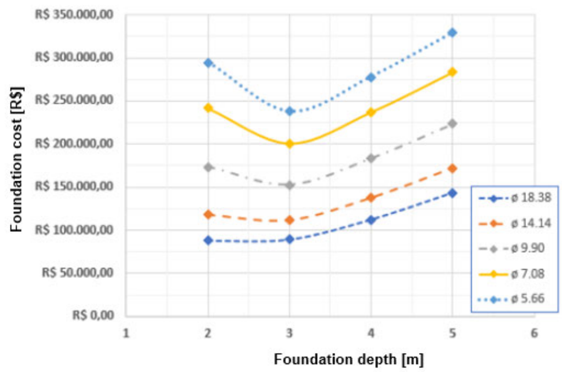

(c) Pentagonal

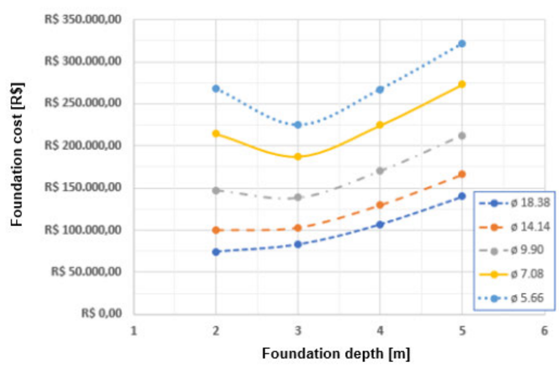

(d) Hexagonal

FIGURE 12. Estimated foundation costs as a function of depth for lattice towers.

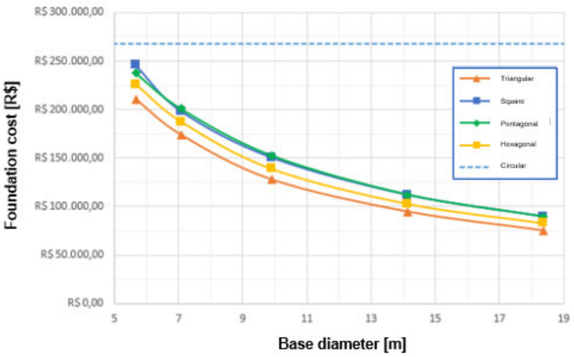

FIGURE 13. Estimated foundation costs for a lattice tower (3 m depth) and a circular tower (fixed foundation diameter of 14.8 m).

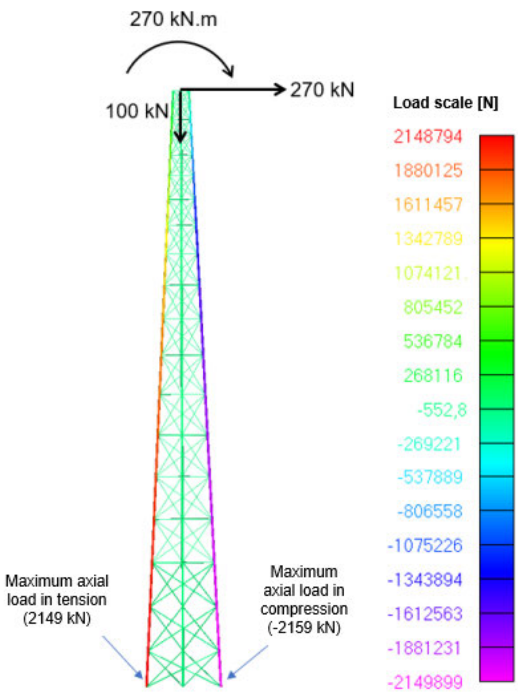

FIGURE 14. Axial load distribution in the triangular tower (3D FEA).

C. PERFORMANCE AND AERODYNAMIC OPTIMIZATION

The triangular lattice tower, with a minimal frontal area, significantly reduces load fluctuations on the blades, promoting greater energy capture and noise suppression. Oblong horizontal elements (Figure 16) and conductor tubes along the tower legs were used to energize the boundary layer and disrupt Von Kármán vortices, mitigating the wake interference with the downwind-positioned rotor. These conductor tubes also contribute to the reduction of aerodynamic interference, optimizing the turbine's performance.

Solid steel bars were used as diagonal elements in the section of the tower located ahead of the rotor, with the aim of reducing the frontal area and minimizing the interference of the structure with the airflow reaching the rotor, positioned downwind. This variation in diagonal elements is illustrated in Figure 15.

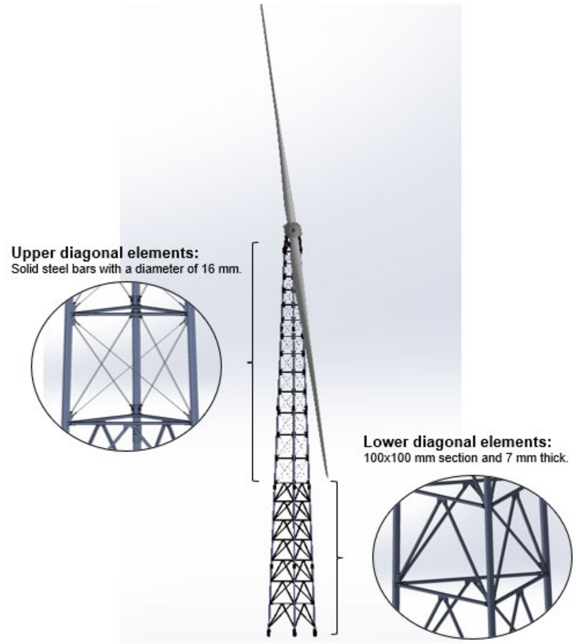

FIGURE 15. Variation of diagonal elements in the tower.

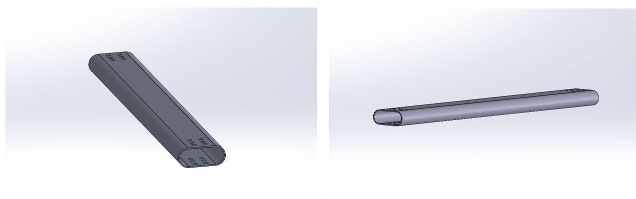

FIGURE 16. Horizontal elements with oblong cross-section.

D. FINAL DESIGN

The triangular lattice tower with an 8.12 m base diameter and 58.37 m height was finalized, adjusting the original 10-12 m base range to address two key challenges: the increase in nacelle mass and issues related to the availability of components in the Brazilian market. Initially, the nacelle was designed to weigh 6 tons, but design changes led to an increase in mass to 25 tons, which significantly reduced the tower's frequency and brought it dangerously close to the rotor blade passage frequency (0.7 Hz). This situation posed a potential risk of resonance and structural failure. To mitigate this, the base diameter was adjusted to maintain structural stability.

Furthermore, the original components specified for the tower, particularly those needed for a 10 m base diameter design, were not widely available in the Brazilian market. This led to several complications, including:

- Difficulty in acquiring the necessary components within the project's time frame and budget.

- The need for large order quantities, which were incompatible with the project's schedule.
- High costs associated with custom manufacturing and limited availability of certain parts.

As a result, the decision was made to adjust the tower's dimensions to 8.12 m in base diameter to address both the increase in nacelle mass and the challenges posed by component availability. Two strategies were evaluated (Table 4): increasing the tower's rigidity, which raised costs, or reducing rigidity (through thinner components and taller height), which helped balance safety and feasibility.

The final design is a triangular lattice tower (8.12 m base, 58.37 m height) optimized for Class III-B conditions. Loads were derived from IEC 61400-1 cases 2.1 (power production failure) and 3.3 (startup transient). The tower comprises:

- **Vertical Tubes**: ASTM A501 Grade B, 323.8 mm diameter, 10 mm thick (Figure 18).
- **Horizontal Tubes**: ASTM A500, 168.3 mm diameter, 7.1 mm (lower), 5.16 mm (upper) (Figure 18).
- **Diagonal Elements**: NBR 8261 Grade B, 100 × 100 mm, 7 mm thick (lower); AISI 4140, 16 mm solid bars (upper) (Figure 18).
- **Hardpoints**: ASTM A572 Grade 50, welded to vertical tubes, connected via bolts/pins (Figure 17).

Welding used SMAW/GMAW with prequalified fillers (Table 5). Modal analysis confirmed first-mode frequencies of 0.505-0.553 Hz, below the 0.7 Hz blade passing frequency.

E. FATIGUE ANALYSIS

Fatigue analysis was conducted using Mlife software, which incorporates classical fracture mechanics theories, including the Goodman correction, Palmgren-Miner rule, and Basquin's equation. The analysis also employed the rainflow counting method for cycle counting and calculated damage by summing the damage from each load. This approach ensured adequate performance, particularly in the context of fracture mechanics, where components are designed to withstand loads without catastrophic failure.

The focus of joint performance was on welds, as bolted joints were designed to avoid fatigue, provided the external forces do not exceed the preload or frictional force. A damage-tolerant design philosophy was adopted for the welds, meaning that crack nucleation could occur during the operational life of the machine. This approach necessitates a comprehensive inspection and maintenance program, including regular monitoring of welded joints to assess crack propagation and determine whether the crack length approaches the critical crack size. Scheduled inspections will be conducted to evaluate the integrity of the welds, and maintenance actions will be promptly taken if necessary. Should the crack length exceed the critical value, the weld must be removed, cleaned, and rewelded to restore the joint's integrity and ensure the long-term durability of the structure.

The results of the analysis indicated that the shortest estimated life for a welded joint was 8 years, while others

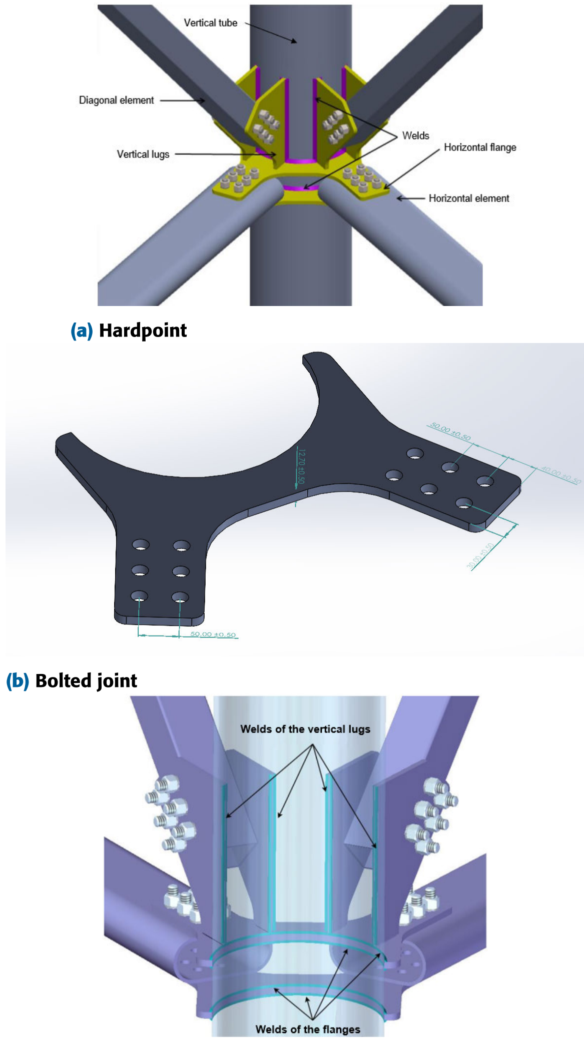

(a) Hardpoint

(b) Bolted joint

(c) Fillet weld

FIGURE 17. Joint designs for the ABV tower.

demonstrated a service life of over 20 years. To provide additional safety in case of weld failure, reinforcements at the joints (Figure 19) were incorporated. These reinforcements are designed to prevent catastrophic failure structure by providing additional support, thereby improving the overall safety and durability of the structure.

F. LOGISTICAL CONSIDERATIONS

A pivot system was developed with the goal of reducing assembly and logistics costs, which are typically impacted by the rental of heavy equipment such as cranes and the transportation of large, bulky structures that often require escort vehicles. By eliminating the need for these resources, a more cost-effective solution was achieved. The pivoting feet system (Figure 21) allows the tower to be assembled directly on-site in a horizontal position. This method eliminates the need for moving large pre-assembled modules, significantly reducing transportation costs.

TABLE 4. Comparison of redesign strategies for the triangular tower.

Criterion	Option A: Increase Rigidity	Option B: Reduce Rigidity
Premise	Raise frequency above 0.7 Hz	Lower frequency below 0.7 Hz
Solution	Thicker components, shorter height, larger base	Thinner components, taller height, smaller base
Advantages	Standardized components, less material (shorter height)	Lighter structure, standardized components
Challenges	Higher weight/costs, blade clearance risk, overdesign	More material (taller), buckling risk (smaller base)

TABLE 5. Filler metal specifications for welding.

Base Metal	SMAW	GMAW
ASTM A500 Grade B/C	E60XX, E70XX	ER 70S-X
ASTM A501 Grade B, A572 Grade 50	E7015, E7016, E7018, E7028	ER 70S-X, E70C-XC, E70C-XM

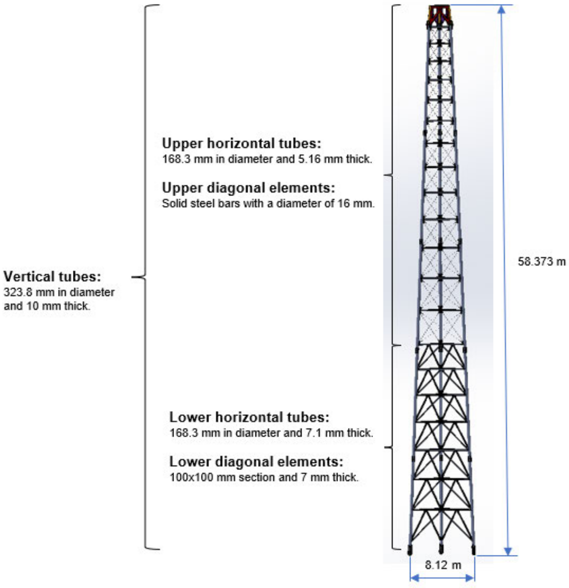

FIGURE 18. Detailed specification of tower element dimensions.

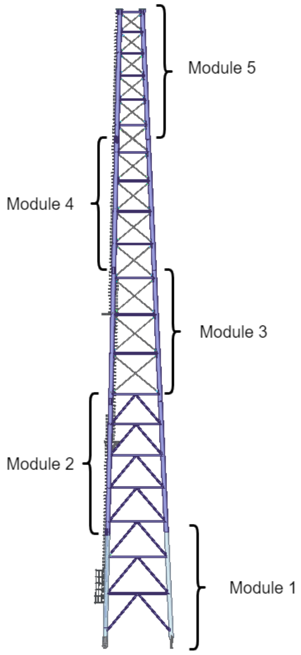

FIGURE 20. ABV tower modules.

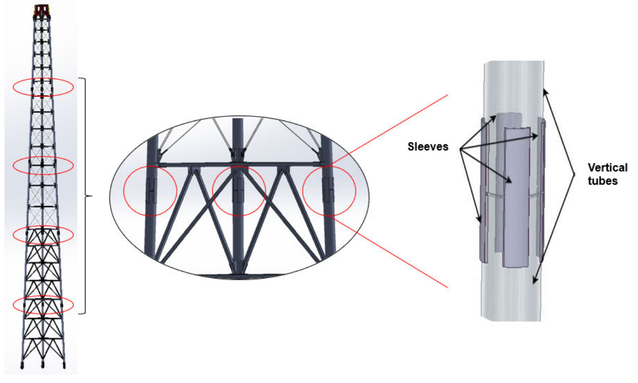

FIGURE 19. Reinforcements for tower joints.

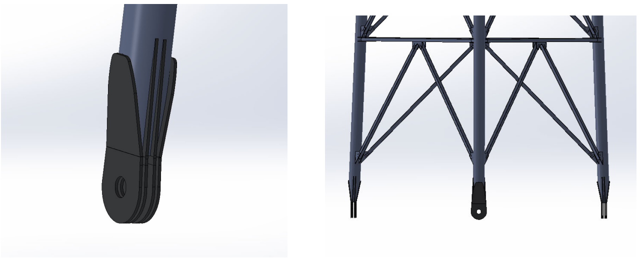

(a) Pivot foot **(b)** Assembly

FIGURE 21. Pivot system for horizontal assembly of the tower, designed to reduce logistics costs and allow assembly directly on-site before being raised to the vertical position.

Assembling the structure horizontally also offers operational advantages, including faster and more efficient welding under favorable conditions. Once the assembly is complete, the structure is raised to a vertical position using a cable

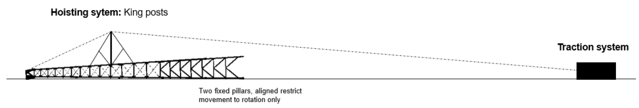

FIGURE 22. Tower lifting process.

and drum system anchored to foundation pillars, with a 132 mm pin ensuring stability during the lifting process (Figure 22).

This tower hoisting and assembly system is still in development, aiming to provide an efficient, cost-effective solution for overcoming the challenges of transportation and assembly in remote areas, such as those encountered in Brazil. The tower was segmented into five modules (Figure 20) to facilitate the assembly process and to address Brazil's specific transportation constraints.

IV. CONCLUSION AND FUTURE WORK

The ABV lattice tower presents a cost-effective, structurally robust, and aerodynamically efficient solution for Brazil's low-wind regions. The triangular configuration (8.12 m base, 58.37 m height) offers significant advantages, including a 40% reduction in weight, 60% decrease in frontal area, and 50% reduction in foundation costs compared to traditional circular towers, while ensuring dynamic stability within frequencies of 0.505-0.553 Hz.

This design solution arose from a thorough finite element analysis (FEA) that considered structural stresses, aerodynamic optimization based on the downwind rotor configuration, and logistical constraints such as transportation and on-site assembly. The lattice tower typology was chosen for its superior cost-benefit ratio, outperforming tubular towers in terms of weight, cost, and structural efficiency. In addition, standardized manufacturing processes were employed to streamline fabrication, simplifying field welding and eliminating preheating.

Despite these advantages, some limitations remain. Rotor clearance analysis in accordance with IEC 61400-1 and long-term fatigue monitoring are necessary, as the weld life (estimated at 8-20 years) requires ongoing maintenance. Future work will focus on integrating rotor design, and incorporating IoT sensors for real-time fatigue monitoring to enhance performance and durability.

A key aspect still under development is the tower hoisting system, which, once finalized, will significantly reduce transportation and assembly costs. This system will eliminate the need for heavy cranes and escort vehicles, allowing for horizontal on-site assembly and offering a cost-effective solution for remote locations. Ultimately, this innovation will lead to major reductions in logistical and installation costs, further optimizing the entire project's feasibility and economic efficiency.

REFERENCES

[1] Agência Nacional de Energia Elétrica. (2025). *Resultado Dos Leilões De Geração No Ambiente Regulado*. [Online]. Available: https://www.gov.br/aneel/pt-br/centrais-de-conteudos/relatorios-e-indicadores/geracao

[2] Empresa de Pesquisa Energética. (2024). *Consumo Mensal De Energia Elétrica Por Classe (Regiões E Subsistemas)*. [Online]. Available: https://www.epe.gov.br/pt/publicacoes-dados-abertos/publicacoes/consumo-de-energia-eletrica

[3] Instituto brasileiro de geografia e Estatística. (2022). *Sistema De Contas Regionais*. [Online]. Available: https://www.ibge.gov.br/estatisticas/economicas/contas-nacionais/9054-contas-regionais-do-brasil.html?edicao=41862&t=resultados

[4] L. Lledó, V. Torralba, A. Soret, J. Ramon, and F. J. Doblas-Reyes, "Seasonal forecasts of wind power generation," *Renew. Energy*, vol. 143, pp. 91–100, Dec. 2019.

[5] *Wind Energy Generation Systems—IEC 61400 Part 1: Design Requirements*, International Electrotechnical Commission, Geneva, Switzerland, 2019.

[6] C. J. Sudhakar, D. R. Joshi, and N. R. Chitragar, "A review on design of low wind speed wind turbines," *Int. J. Innov. Res. Electr., Electron., Instrum. Control Eng.*, vol. 7, no. 12, pp. 23–28, 2019. [Online]. Available: https://ijireeice.com/papers/a-review-on-design-of-low-wind-speed-wind-turbines/

[7] International Renewable Energy Agency (IRENA), Abu Dhabi, United Arab Emirates. (Jun. 2016). *The Power to Change: Solar and Wind Cost Reduction Potential To 2025*. [Online]. Available: https://www.irena.org/-/media/Files/IRENA/Agency/Publication/2016/IRENA_Power_to_Change_2016.pdf

[8] J. Yacoubou. (Mar. 2022). *Utility and Residential Wind Turbine Costs Explained*. GreenCoast. Accessed: Sep. 20, 2022. [Online]. Available: https://greencoast.org/wind-turbine-costs

[9] S. Krohn, P. E. Morthorst, and S. Awerbuch. (Mar. 2009). *The Economics of Wind Energy*. European Wind Energy Association (EWEA), Brussels, Belgium. [Online]. Available: https://www.ewea.org/fileadmin/ewea_documents/documents/00_POLICY_document/Economics_of_Wind_Energy__March_2009_.pdf

[10] International Renewable Energy Agency (IRENA). (Jun. 2017). *Renewable Energy Benefits: Leveraging Local Capacity for Onshore Wind*. [Online]. Available: https://www.irena.org/-/media/Files/IRENA/Agency/Publication/2017/Jun/IRENA_Leveraging_for_Onshore_Wind_Executive_Summary_2017.pdf

[11] P. van der Male, R. van Schaik, M. Vergassola, and K. N. van Dalen, "Tower shadow excitation of a downwind rotor blade of a turbine with a tubular tower," *J. Phys., Conf. Ser.*, vol. 1618, no. 3, Sep. 2020, Art. no. 032019.

[12] T. Wang and F. N. Coton, "A high resolution tower shadow model for downwind wind turbines," *J. Wind Eng. Ind. Aerodyn.*, vol. 89, no. 10, pp. 873–892, Aug. 2001.

[13] M. Robinson, D. R. GalbraithShipley, and M. Miller, "Unsteady aerodynamics of wind turbines," in *Proc. 33rd Aerosp. Sci. Meeting Exhib.*, Jan. 1995, pp. 1–12.

[14] L. K. Gan, J. K. H. Shek, and M. A. Mueller, "Modeling and characterization of downwind tower shadow effects using a wind turbine emulator," *IEEE Trans. Ind. Electron.*, vol. 64, no. 9, pp. 7087–7097, Sep. 2017.

[15] A. B. de Normas Técnicas, "NBR6123: Forças devidas ao vento em edificações," ABNT—Associação Brasileira de Normas Técnicas, São Paulo, SP, Brazil, Tech. Rep. NBR 6123, 1988.

[16] *Specification for Structural Steel Buildings (ANSI/AISC 360-16)*, Amer. Inst. Steel Construct., Chicago, IL, USA, 2016.

[17] *Projeto De Estruturas De Aço E De Estruturas Mistas De Aço E Concreto De Edifícios*, Standard NBR 8800, Rio de Janeiro, Associação Brasileira de Normas Técnicas, 2014.

[18] American Society of Civil Engineers. (2013). *(ASCE-SEI 7-10: Minimum Design Loads for Buildings and Other Structures*. [Online]. Available: https://ascelibrary.org/doi/abs/10.1061/9780784412916

[19] *Structural Welding Code—Steel (AWS D1.1)*, American Welding Society, Doral, FL, USA, 2015.

[20] *Eurocode 3: Design of Steel Structures—Part 1–8: Design of Joints*, Standard EN 1993-1-8, 2005.

JAMES ROJAS WATERHOUSE received the B.Sc. degree in mechanical engineering with emphasis on aircraft, the M.S. degree in engineering, and the Ph.D. degree in aeronautical renewable fuels from the University of São Paulo, Brazil, in 1995, 2000, and 2010, respectively. He is currently a Researcher and Tenured Professor with the Department of Aeronautical Engineering, São Carlos School of Engineering, USP. His research interests include wind energy, composite materials, aircraft design, and certification.

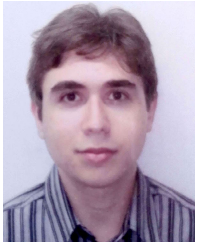

CARLOS HENRIQUE GASPARETTI received the B.Sc. degree in aeronautical engineering from the University of São Paulo, Brazil, in 2025. He is currently an Engineer in aerodynamics and aeroacoustics area with Newco Blades Technology. His research interests include renewable energy, design engineering, and fluid dynamics.

KAUAN PIRES QUEVEDO is currently pursuing the degree in mechanical engineering with the University of São Paulo, Brazil. His research interests include heat transfer, thermodynamics, and wind energy.

GUILHERME BEPPU DE SOUZA received the B.Sc. degree in aeronautical engineering from the University of São Paulo, Brazil, in 2024. He is currently an Engineer in aerodynamics and dynamics area with Newco Blades Technology. His research interests include wind energy, dynamic simulations, and multidisciplinary optimization.

Coordenação de Aperfeiçoamento de Pessoal de Nível Superior (CAPES) - ROR identifier: 00x0ma614